IKZF1/3 and CRL4-CRBN E3 ubiquitin ligase mutations and IMiD resistance in multiple myeloma

by Santiago Barrio, Umair Munawar, Yuan Xiao Zhu, Nicola Giesen, Chang-Xin Shi, Matteo Da Viá, Richard Sanchez, Laura Bruins, Theresa Demler, Nicole Müller, Larissa Haertle, Andoni Garitano, Torsten Steinbrunn, Sophia Danhof, Isabel Cuenca, Clara Barrio-Garcia, Esteban Braggio, Andreas Rosenwald, Joaquin Martinez-Lopez, Leo Rasche, Marc S. Raab, A. Keith Stewart, Hermann Einsele, Thorsten Stühmer, and K. Martin Kortüm

IKZF1/3 and CRL4^{CRBN} E3 ubiquitin ligase mutations and IMiD resistance in multiple myeloma

Santiago Barrio[1], Umair Munawar[2], Yuan Xiao Zhu[3], Nicola Giesen[4], Chang-Xin Shi[3], Matteo Da Viá[1], Richard Sanchez[5], Laura Bruins[3], Theresa Demler[2], Nicole Müller[1], Larissa Haertle[1], Andoni Garitano[1], Torsten Steinbrunn[1], Sophia Danhof[1], Isabel Cuenca[5], Clara Barrio-Garcia[6], Esteban Braggio[3], Andreas Rosenwald[7], Joaquin Martinez-Lopez[5], Leo Rasche[1], Marc S. Raab[4], A Keith Stewart[3,8], Hermann Einsele[1], Thorsten Stühmer[2], and K Martin Kortüm[1]

[1]Department of Internal Medicine II, University Hospital of Würzburg, Würzburg, Germany.

[2]Comprehensive Cancer Center Mainfranken, University Hospital of Würzburg, Würzburg, Germany.

[3]Department of Hematology, Mayo Clinic, Scottsdale, AZ, USA.

[4]Department of Internal Medicine V, Heidelberg University Hospital, Heidelberg, Germany, and CCU Molecular Hematology/Oncology, German Cancer Research Center (DKFZ).

[5]Hematology Department Hospital 12 de Octubre, Complutense University, H12O-CNIO Clinical research unit, CIBERONC Madrid, Spain.

[6]Gene Center, Ludwig-Maximilians University, Munich, Germany.

[7]Institute of Pathology, University of Würzburg, Würzburg, Germany.

[8]Center for Individualized Medicine of the Mayo Clinic, Rochester, USA.

Correspondence:

Priv.-Doz. Dr. K. Martin Kortüm

Department of Hematology and Oncology

University Hospital of Würzburg

Germany

Email: kortuem_m@ukw.de

Cereblon (CRBN), target of immunomodulatory drugs (IMiDs), forms the CRL4[CRBN] E3 ubiquitin ligase (CRL4) complex with DDB1, CUL4B and ROC1.[1,2] Under the influence of IMiDs, CRL4 polyubiquitinates and thus depletes the transcription factors IKZF1 and IKZF3, resulting in cytotoxicity to multiple myeloma (MM) cells. In vitro, CRBN and IKZF1/3 mutations affecting the CRBN-Lenalidomide (LEN) binding site (degron) cause drug resistance to IMiDs.[3–5] Here, we hypothesized that mutations in the other components of the CRL4 complex and its targets Ikaros and Aiolos likewise interfere with the ubiquitin ligase activity, thus contribute to IMiD resistance. In order to select the most promising patient derived mutation candidates for functional validation, we first generated a comprehensive overview of point mutations in advanced MM patients affecting *IKZF1*, *IKZF3* or *CRL4* genes. Next, we contextualized all described mutations at the protein level, to investigate their structural impact on complex formation and stability. Based on these analyses, we then selected a subset for functional validation by expressing mutant IKZF1, CRBN or CUL4B in MM cell lines and analyzed their effects on resistance to IMiDs, thus probing the relevance of such alterations for complex integrity and the transmission of IMiD activity.

To select relevant mutation candidates, we analyzed data from different Multiple Myeloma Mutation panel (M3P) cohorts[3,6–8] and from other published and unpublished datasets[9,10] for a total of 1,838 MM cases (**Supplemental methods**). In this meta-analysis we observed the mutation frequency increased significantly after treatment (Z-score: 4.5, p<0.00001), from 2.0% (28/1373) in untreated to 6.2% (29/465) in pretreated cases. Notably, this increase occurs predominantly in three genes, *IKZF1* (0.15% to 1.3%, Z-score: 2.9, p=0.001), *CRBN* (0.44% to 2.15%, Z-score: 3.4, p=0.006) and *CUL4B* (0.44% to 1.93%, Z-score: 3.4, p=0.004, **Supplemental figure 1**). 71% (24/34) of the *IKZF1/3*, *CRBN*, *DDB1*, *CUL4B* and *ROC1* mutations found in treated patients were nonsense or located within previously described binding areas, whereas at diagnosis the distribution was spread out all along the gene loci[2,4,11] suggesting passenger mutations. We identified three potential new hotspots (IKZF3 G159R/A, IKZF1 A152T and CUL4B R820T/S) each represented by mutations in two different patients. All the detected mutations and variant read frequencies (VRF) are summarized in **Supplemental table 1**. Of interest, in eight patients with sampling available from diagnosis and relapse, *CRBN* and *CUL4B* mutations were acquired after IMiD treatment, whereas *IKZF3* mutations were also identified in *de novo* disease (**Supplemental figure 1**). Together, these results suggest that CRL4 mutations play an important role in disease progression and clonal evolution.

Next, we functionally assessed effects of patient-derived mutations in Ikaros and Aiolos. We constructed Sleeping Beauty vectors for expression of four IKZF1 mutations (A152T, E170D, Y413C and R439H), and for one in IKZF3 (G159R) (**Figure 1A**), and stably introduced these into MM cell lines (MM1.S and L363: IMiD sensitive, AMO1: less sensitive). Whereas this led to strong expression for all IKZF1 constructs, the IKZF3 expression vectors (WT and G159R), unfortunately, did not lead to noticeable expression even though two different versions using either CMV- or CAAG-driven expression cassettes, were tested (**Supplemental figure 2**). Viability assessments for all L363 IKZF1 sub-lines after six-day-treatment with 10 µM LEN showed that exclusively the mutation at the LEN binding site (A152T) conferred resistance to the drug (**Figure 1B, top**). This observation was supported by Western blotting, which showed that only in A152T subline overnight treatment with LEN was without effect on the level of Ikaros (**Figure 1B, bottom**). Furthermore, a minor inhibitory effect on IKZF1 degradation was also observed for the mutation E170D, which is located within close proximity of the degron sequence. This result was confirmed in cell lines AMO-1 (**Supplemental figure 2B**) and MM1.S (not shown). However, the slightly enhanced levels of IKZF-E170D after LEN treatment did not lead to measurable changes in cell viability and apoptosis assays. In order to investigate the biological effects of IKZF1-E170D on proliferation fitness under Len treatment, we employed a clonal competition assay (CCA) and

tested L363 co-cultures of fluorescently-identifiable sublines (IKZF1-WT vs IKZF-A152T, IKZF-E170D or IKZF-R439H) growing under the selective pressure of a modest concentration of LEN (2,5 µM, **Supplemental methods**). Of note, IKZF1-A152T cells had a significant survival advantage compared to IKZF1-WT cells. Complete dominance in the culture (inversion from an initial ratio of 10% mut/90% WT to 90% mut/10 % WT) was observed after 21 days in co-culture. No such effect was observed for IKZF-E170D and IKZF-R439H cells (**Figure 1C**), which is in line with published data, that exclusively mutations affecting the IKZF1 degron sequence[4] induce IMiD resistance.

We previously demonstrated that loss of CRBN or the occurrence of mutations at the IMiD binding site of CRBN induce resistance to immunomodulatory drugs.[3] However, 56% of the missense *CRBN* mutations did not affect the IMiD binding pocket, but were present in the previously described CRBN Lon-like domain (LLD; residues 76-318), that contains a DDB1-binding motif (**Figure 2A**).[11] Furthermore, *in silico* analysis[12] suggests that 7 of 9 mutations affect this region (P85S, R111Q, F120V, D291N, L308F, R309H and I314S), thus may lead to a reduction of CRBN stability (predicted stability change $\Delta\Delta G<0$, **Supplemental table 1**). To understand whether these alterations also affect IMID sensitivity, we selected two *CRBN* mutations detected in IMID resistant patients (R309H and L190F) and lentivirally introduced them into OCIMY5 cells (cells that have very low levels of endogenous CRBN expression and, thus are resistant to IMiDs). As shown in **Figure 2B**, both types of CRBN mutant-transduced cells showed a substantial reduction of sensitivity to LEN compared with WT CRBN transduced cells. However, further immunoblotting indicated that exogenous CRBN expression in the mutant-transfected cells was much lower than in WT CRBN transduced cells. In order to analyze whether this effect was related to intrinsic features of the mutations, we performed a titration of WT CRBN virus (1000 virus equivalents to 75) and found that a decrease of virus equivalents correlates with decreases in RNA and protein levels of CRBN in the infected MM cells. Although both CRBN mutant virus preparations show the highest virus equivalents, and although this corresponds to high levels of expressed CRBN RNA in OCIMY5 cells, these cells fail to express equivalent levels of CRBN protein (**Figure 2C**). These results suggest that in addition to CRBN mutations in the IMiD binding site other point mutations may play a role in IMiD resistance development either through impaired binding with other proteins of the complex or through destabilizing effects on the protein.

We also hypothesized that mutations in DDB1, CUL4B and ROC1 may affect the formation of the CRL4 complex (**Figure 3A**). To confirm this, we prepared a CUL4B KO model (in L363 cells) using the CRISPR/Cas9 system. Of 10 viable clones, we selected one with clear KO of CUL4B (**Figure 3B, top**). The KO clone was more resistant to LEN treatment compared to the naïve L363 cells. This effect was confirmed by clonal competition assay, in which an advantage in survival fitness under the selective pressure of Len was observed for the CUL4B KO clone compared to the CUL4B WT cells (**Figure 3B, bottom left**). The clonal dynamics become even clearer when both CUL4B KO and WT cells are initially present in equal amounts and cultured without LEN. The wildtype cells easily outcompete the CUL4B KO clone under these conditions, but once the drug is added (2,5 µM, at day 21 in co-culture) the resistant clone takes over (**Figure 3B, bottom right)**. Of note, the re-introduction of WT CUL4B into the CUL4B knockout cells re-sensitized the cells to LEN, confirming our hypothesis. Likewise, reintroduction of two other CUL4B mutants from IMiD pretreated patients (D311H, and R820S, a hotspot mutation detected in two MM patients) also reverted the resistance, suggesting that these two mutations do not alter the response to IMiDs (**Supplemental figure 3**).

We confirmed an increase of mutations in *CRBN*[3] and detected similar results for *CUL4B* and *IKZF1* after therapy. In eight cases of our cohort with acquired mutations within the CRL4 complex, a prior tumor sample was available (diagnosis-progression/relapse). In these sequential samples *CRBN* and *CUL4B* mutations were acquired after IMiD exposition, in

contrast, alterations in *IKZF3* were already detectable at diagnosis. This suggests that *IKZF3* mutations might play a role in the pathogenesis of MM rather than in therapy-induced resistance development. Recently, CRBN protein loss and point mutations in the CRBN-LEN binding area were associated with IMiD resistance.[3] Mutations in the CRBN-DDB1 binding motif[11] may also induce resistance to LEN (**Figure 2B**). However, the underlying mechanisms of the mutations investigated were not related to binding, but may lead to the destabilization of the protein folding that induces CRBN degradation (**Figure 2C**). The KO by CRISPR/Cas9 of CUL4B induced resistance to LEN, highlighting the importance of this protein for the anti-tumor action of IMiDs. The fact that this resistance was overcome by the reintroduction of CUL4B WT using Sleeping Beauty proved the specificity of our in vitro approach (**Figure 3B**).

This is the first comprehensive analysis of CRL4 point mutations on the impact of IMiD responses in MM. Mutations are predominantly selected for by therapy and affect the function of the ubiquitin ligase complex through loss of a subunit by nonsense mutation, point mutations affecting protein stability, or by impairment of substrate binding. Some alterations, including *IKZF3* hotspot mutations, are detectable prior to treatment at initial diagnosis. The possible implications of such alterations in the pathophysiology of MM deserves further investigation.

References

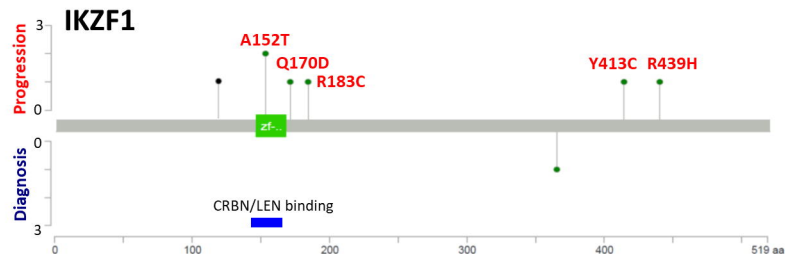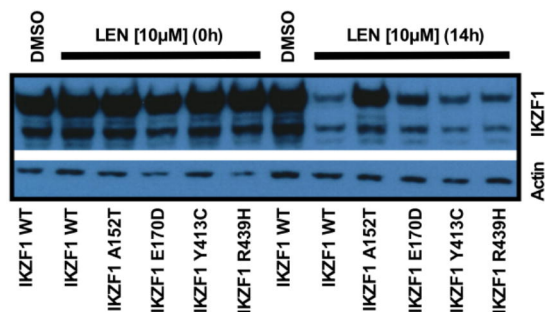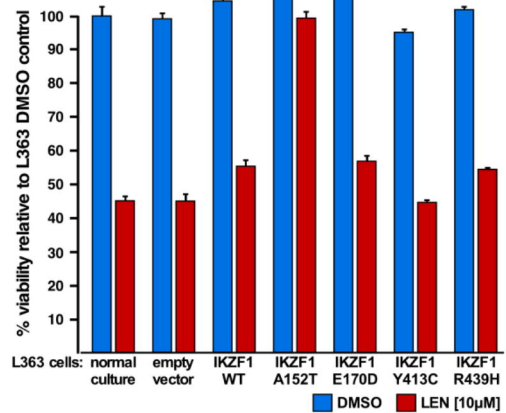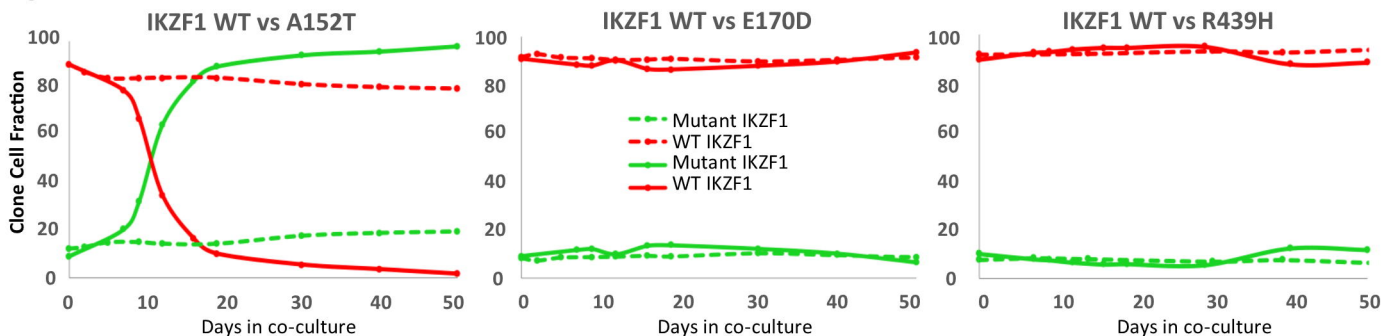1. Kortum KM, Zhu YX, Shi CX, Jedlowski P, Stewart AK. Cereblon binding molecules in multiple myeloma. Blood Rev. 2015;29(5):329-334.

2. Fischer ES, Scrima A, Bohm K, et al. The molecular basis of CRL4DDB2/CSA ubiquitin ligase architecture, targeting, and activation. Cell. 2011;147(5):1024-1039.

3. Kortum KM, Mai EK, Hanafiah NH, et al. Targeted sequencing of refractory myeloma reveals a high incidence of mutations in CRBN and Ras pathway genes. Blood. 2016;128(9):1226-1233.

4. Kronke J, Udeshi ND, Narla A, et al. Lenalidomide causes selective degradation of IKZF1 and IKZF3 in multiple myeloma cells. Science 2014;343(6168):301-305.

5. Zhu YX, Braggio E, Shi C-X, et al. Identification of cereblon-binding proteins and relationship with response and survival after IMiDs in multiple myeloma. Blood. 2014;124(4):536-545.

6. Kortuem KM, Braggio E, Bruins L, et al. Panel sequencing for clinically oriented variant screening and copy number detection in 142 untreated multiple myeloma patients. Blood Cancer J. 2016;6(2):e397.

7. Kortum KM, Langer C, Monge J, et al. Longitudinal analysis of 25 sequential sample-pairs using a custom multiple myeloma mutation sequencing panel (M(3)P). Ann Hematol. 2015;94(7):1205-1211.

8. Kortum KM, Langer C, Monge J, et al. Targeted sequencing using a 47 gene multiple myeloma mutation panel (M(3) P) in -17p high risk disease. Br J Haematol. 2015;168(4):507-510.

9. Bolli N, Avet-Loiseau H, Wedge DC, et al. Heterogeneity of genomic evolution and mutational profiles in multiple myeloma. Nat Commun. 2014;5:2997.

10. Lohr JG, Stojanov P, Carter SL, et al. Widespread genetic heterogeneity in multiple myeloma: implications for targeted therapy. Cancer Cell. 2014;25(1):91-101.

11. Chamberlain PP, Lopez-Girona A, Miller K, et al. Structure of the human Cereblon-DDB1-lenalidomide complex reveals basis for responsiveness to thalidomide analogs. Nat Struct Mol Biol. 2014;21(9):803-809.

12. Pandurangan AP, Ochoa-Montaño B, Ascher DB, Blundell TL. SDM: a server for predicting effects of mutations on protein stability. Nucleic Acids Res. 2017;45(W1):W229-W235.

Figure legends

Figure 1: Only *IKZF1/3* mutations affecting the LEN/CRBN binding area induce LEN resistance. A: Location of the mutations within the *IKZF3* and *IKZF1* genes. Lollypop plots of all mutations described in IKZF1 and IKZF3. Blue bar; degron sequence of the LEN binding site. Bottom of the lollypop plot: mutations detected at diagnosis. Top: alterations detected after therapy exposition. Green dots indicate missense and black dots nonsense mutations. **B:** Viability and molecular effects of expression of mutated IKZF1 in L363 cells. **C:** Clonal competition assay (CCA) results for IKZF1-WT (red) vs IKZF-A152T, IKZF-E170D or IKZF1-R439H (green). Dashed line: CAA without drug (10% mutant/90% WT). Solid line: CCA with 2.5 µM LEN.
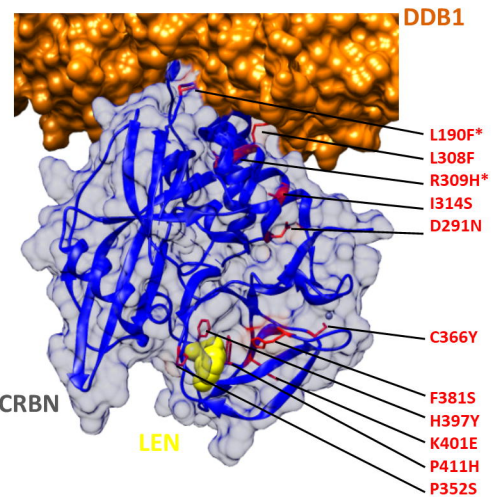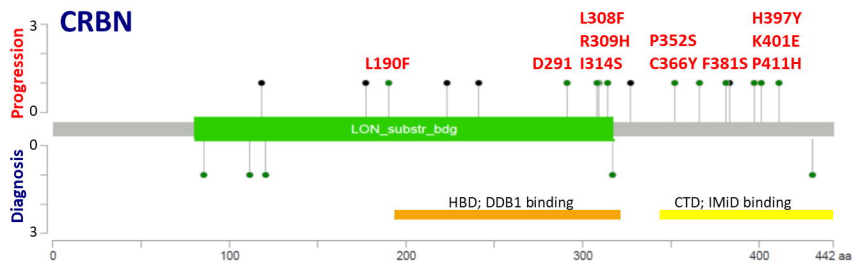
Figure 2: *CRBN* point mutations outside the LEN binding pocket induce protein destabilization. A: *CRBN* mutations at diagnosis and progression. **B:** Viability test analyses (MTT) after 5 day incubation with 5 µM LEN and Western blotting for the different CRBN constructs **C:** Virus titration of the CRBN constructs, compared to RNA expression level (TaqMan assays) and protein quantity (Image).

Figure 3: Loss of CUL4B induces LEN resistance in vitro. A: DDB1, CUL4B and ROC1 mutations in myeloma patients. **B:** Top left: Western blotting of CUL4B WT and KO before and after the introduction of the CUL4B WT or mutant by transfection. Top right: Sequence of the CUL4B KO clone compared to WT. Bottom left: Clonal competition assay (CCA) results for CUL4B KO transformed with CUL4B WT (red) vs CUL4B KO (green). Dashed line: Untreated cells. Solid line: CCA with 2.5 µM LEN. Bottom right: CCA of the same subline combinations without LEN (days 0-21) and after subsequent LEN addition (day 21-40) showing the clonal dynamics induced by the drug.
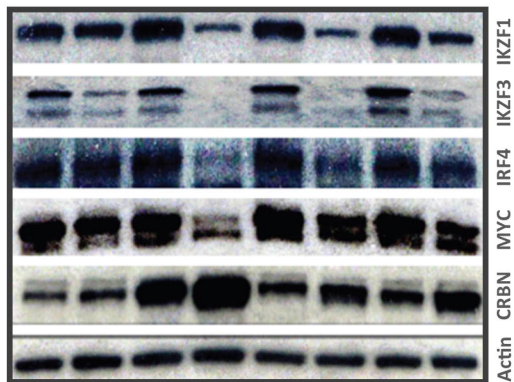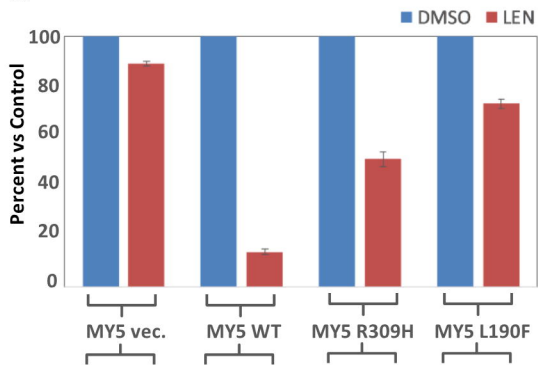
A
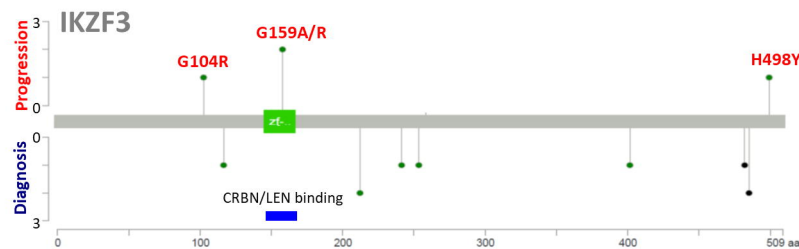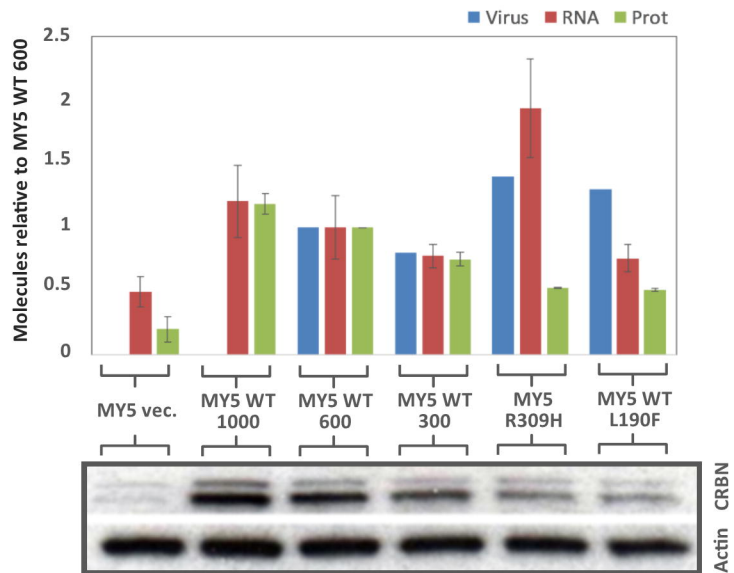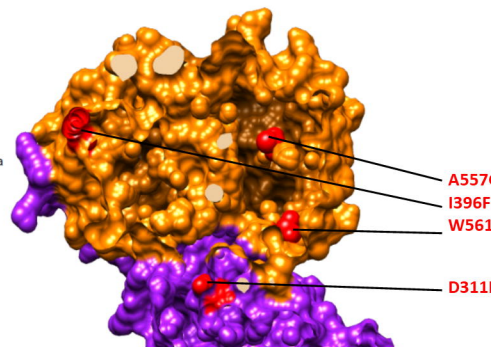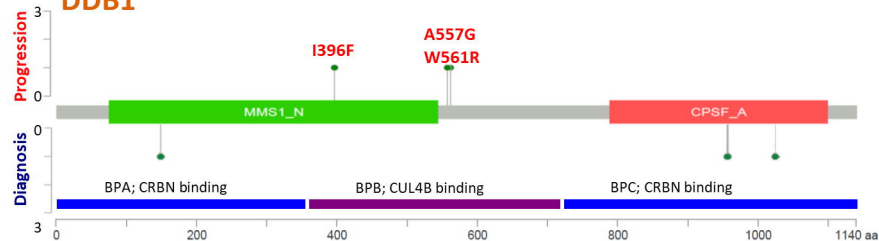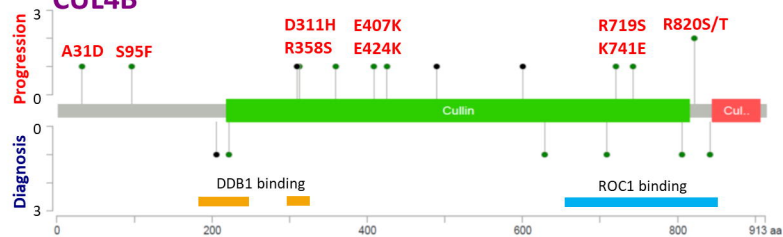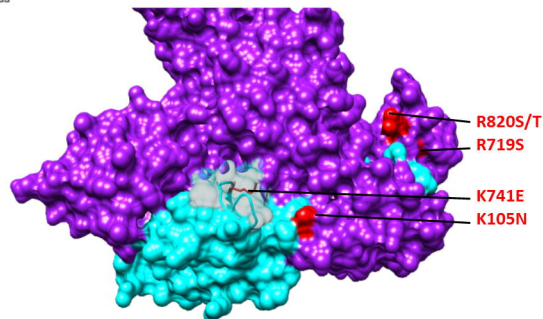
DDB1

I396F

A557G
W561R

MMS1_N

CPSF_A

BPA; CRBN binding   BPB; CUL4B binding   BPC; CRBN binding

0   200   400   600   800   1000   1140 aa

A557G
I396F
W561R
D311H

CUL4B

A31D S95F   D311H E407K   R719S R820S/T
              R358S E424K   K741E

Cullin   Cul..

DDB1 binding   ROC1 binding

0   200   400   600   800   913 aa

R820S/T
R719S
K741E
K105N

ROC1

K105N

zf-rbx1

0   108 aa

B

CUL4B WT   CUL4B KO

+ WT + D311H + R820S   + WT + D311H + R820S

CUL4B

Actin

CUL4B WT   CTGGGGGTTTCAGTGGCTGCTTCCAGCCACGTACCGATACAGAAGAAAGCTGCGTTTTGAAGACACCCTGGAGTTTGTAGGGTTTGATGCGAAGATGGCTGAGGAATCCTCCTCCTCCTCCTCCTCATCTTCACCAA
CUL4B KO   CTGGGG   CTTCACCAA

Supplemental Methods

Meta-analysis

The meta-analysis was restricted to cohorts that include progression samples. Informed consent was obtained according to the declaration of Helsinki in all patients. We pooled 1,373 newly diagnosed MM (NDMM) cases including: Group_1D: 890 cases with WES data available at baseline (CoMMpass IA12 release).[23] Group_2D: own 331 M3P newly diagnosed cases. Group_3D: 152 untreated cases from previously published datasets (WES).[21,22] We compared the incidence in these NDMM groups with progre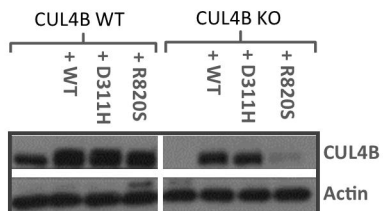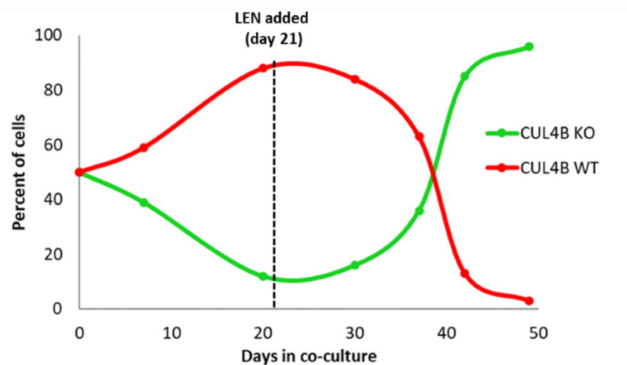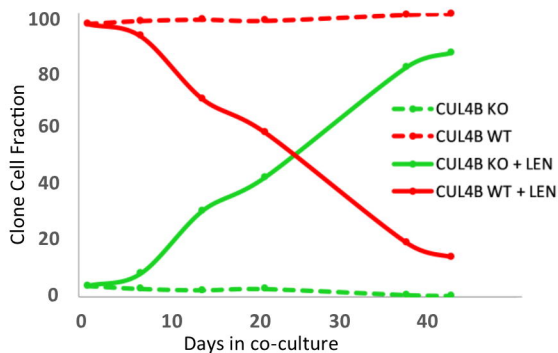ssion samples after therapy (465 cases): Group_1R: 148 WES data from confirmed last relapses in CoMMpass IA12. Group_2R: 164 M3P pretreated cases.[11,18–20], and Group_3R: 115 pretreated cases from previously published datasets.[21,22] Group_4R: 38 WGS advanced, multi-refractory MM cases obtained from a collaboration with the University of Heidelberg (unpublished data).

Targeted deep sequencing

Targeted deep sequencing was performed on paired tumor-germline DNA-samples using the Ion Torrent platform (PGM, Thermo Fisher) and Ion AmpliSeq Library kit. The M3P panel includes in its last version 1,327 amplicons covering the coding regions of 88 myeloma-relevant genes.[24] An average of 759× depth sequencing coverage was generated per nucleotide. Mutation analysis annotation and filtering was performed using Ion Reporter Software v4.4 and screened with the Integrative Genomics Viewer (IGV).[25]

Whole genome sequencing

WGS was performed on MACS sorted CD138+ tumor cells and germline controls. Preparation of DNA libraries was done using the TruSeq DNA Nano kit, sequencing was performed on the HiSeq X using the HiSeq X Ten Reagent kit v2.5 (all Illumina, Hayward, CA) obtaining a median coverage of 77x. Alignment workflow consisted of mapping of raw reads to the human reference genome build 37, version hs37d5, using BWA mem v0.7.8, sorting using SAMtools v0.1.19, and marking of duplicate reads using Sambamba v0.5.9. Somatic SNVs and small indel calling was performed using Mpileup v0.1.19 and Platypus v0.8.1, respectively, and high confidence variants were defined.

Structural analysis

The structural analysis was performed with Chimera 1.11 software[26] and data from public databases (Protein Data Bank). The complete structure of CRL4-CRBN E3 ubiquitin ligase was obtained by merging the structures of LEN-CRBN-DDB1 (PDB_4TZ4) and DDB1-CUL4B-ROC1 (PDB_4A0L), using DDB1 as common polypeptide domain.[7,27] *In silico* prediction of protein stability induced by mutations was performed with the Site Directed Mutator tool.[28]

Site-directed mutagenesis for functional CRBN mutation analysis

To establish mutant CRBN-expressing OCI-MY5 cell lines, we created lentivector pCDHPuroCRBN by subcloning wild-type (WT) CRBN from pCDHGFPCRBN and used this pCDHPuroCRBN as a template to introduce *CRBN* mutations by PCR as we previously described.[11] The ligated plasmid was amplified and isolated by using a Miniprep Plasmid Isolating Kit (QIAGEN) and then cloned into lentivector pCDH-CMV-MCS-EF1-Puro (SBI, Mountain View, CA) and packaged into a lentivirus. The lentivirus expressing WT-CRBN and mutant-CRBN were then used to infect OCI-MY5 myeloma cells to overexpress both WT and mutant CRBN protein. The infected cells were selected with Puromycin for two weeks. The cell viability was assessed in triplicate by using 3-(4,5-dimethylthiazol-2-yl)-2,5-dimethyltetrazolium bromide (MTT) after a 5-day incubation time with different concentrations of LEN.

CUL4B knock out and mutated CUL4B reintroduction

Oligonucleotides for targeting Exon 3 of *CUL4B* gene with the help of CRISPR-Cas9 were designed and cloned into a GeneArt CRISPR nuclease vector (A21175, Thermo Fisher Scientific). L363 cells were co-electroporated with this vector and an expression vector for EGFP, and purified via CD4-microbead selection. Subsequently, undamaged bright green cells were manually picked and seeded into a 96-well plate for clonal upgrowth. Clones were screened for CUL4B status by Western blotting. The exact type of genomic alteration introduced by CRISPR-Cas9 was determined by Sanger sequencing and the complete knockout (KO) of CUL4B protein was verified by Western blotting as described before.[29] CUL4B-WT and CUL4B-mutant (D311H and R820S) protein was then expressed in these KO cells by transposition with Sleeping Beauty (SB) vectors coding for the respective genes. Polyclonal cultures of stable transformants were established by puromycin selection for about 2 weeks and then used in functional experiments such as viability (alamarBlue) and apoptosis assays (annexin V/propidiumiodide)[30], and for Western blotting. For functional experiments in 96-well format 1500 cells per well of either L363 CUL4B-KO, CUL4B-WT or CUL4B-mutant cells were seeded and treated with 10 µM LEN for 6 days.

Clonal competition assays

To characterize the induction of cell resistance over time by the selected mutations in isogenic cells, we established a clonal competition assay system (CCA) using again a SB approach but with G418 selection to stably transfect L363 cells with EGFP and/or LSS mKate RFP. Briefly, after establishment of stably transfected polyclonal cultures of CUL4B mutant / WT marked with different fluorescence proteins, we mixed 90% of "reference-EGFP" cells with 10% of the "mutant-RFP" sub-line and co-cultured them for 40-60 days in the presence or absence of LEN. All experiments were conducted in triplicate to rule out that the observed effects were the result of coincidental alterations acquired over the long culture period. In addition, reference/mutant EGFP/RFP fluorescence was switched in one of the replicates to confirm that the effects are not related to the presence of any specific fluorescent protein. The ratio of EGFP and RFP cells was determined every 4-10 days by flow cytometry, and Sanger sequencing confirmed the genetic integrity of the mutants at the end of the experiment.

A

B

C

Supplemental figure 1
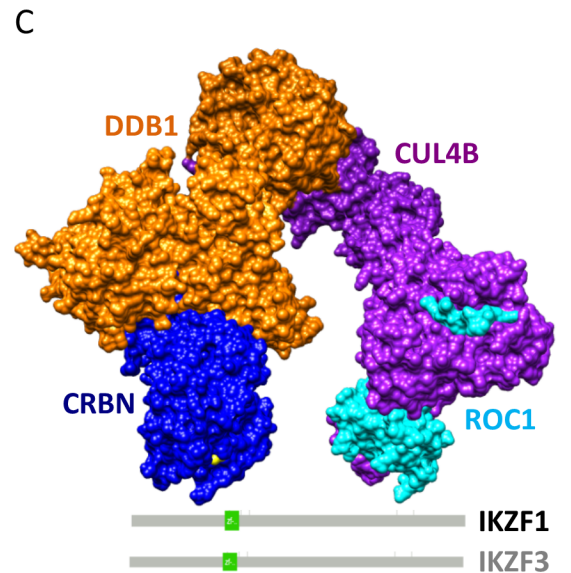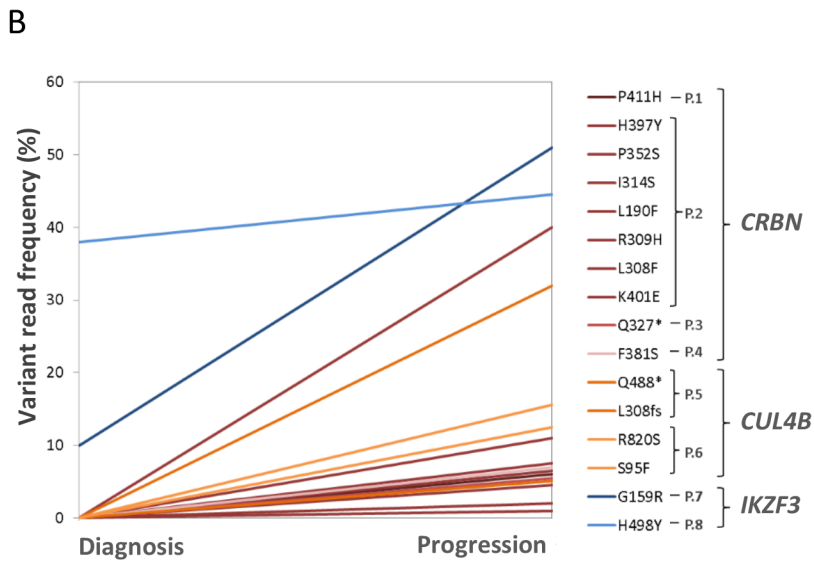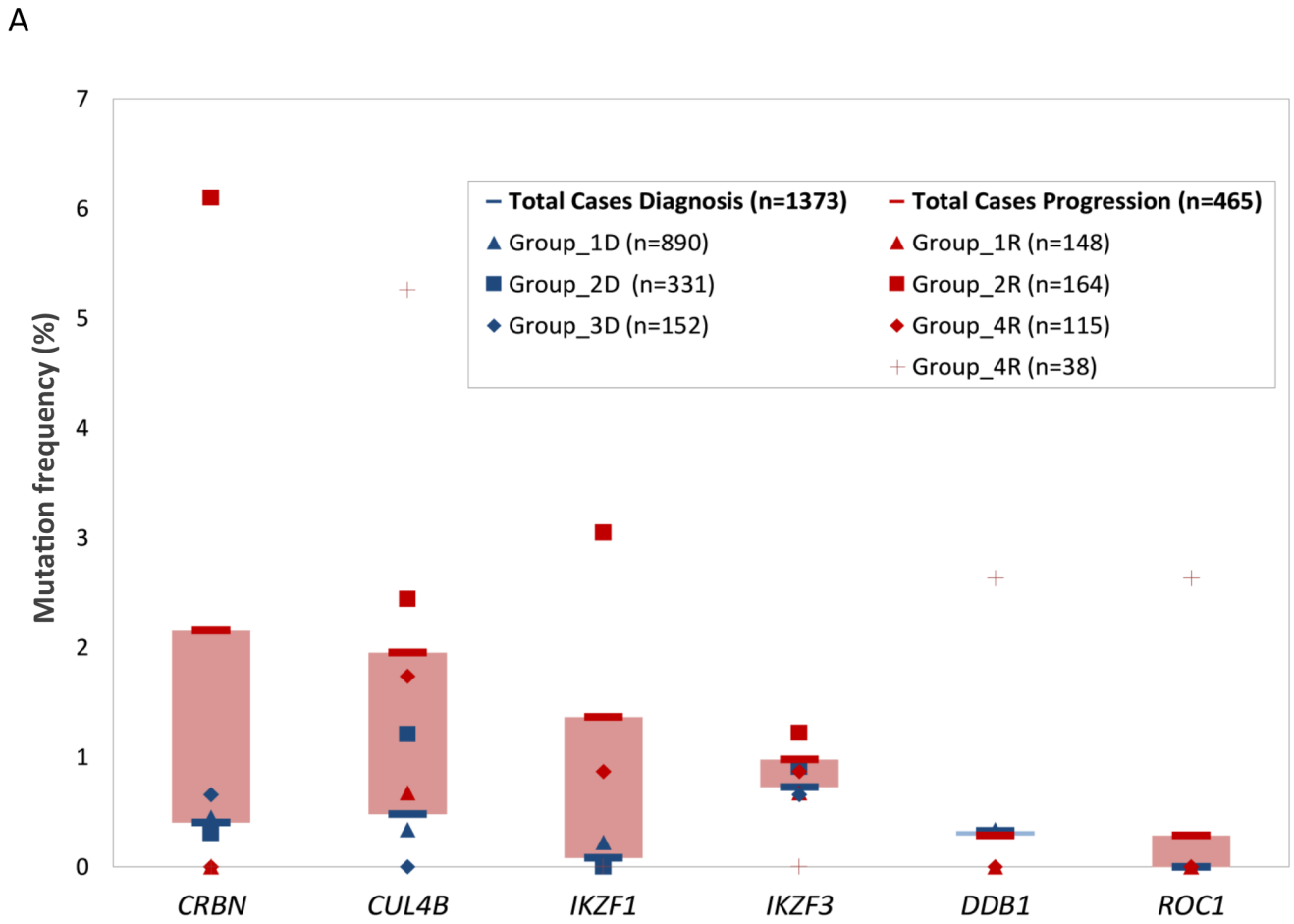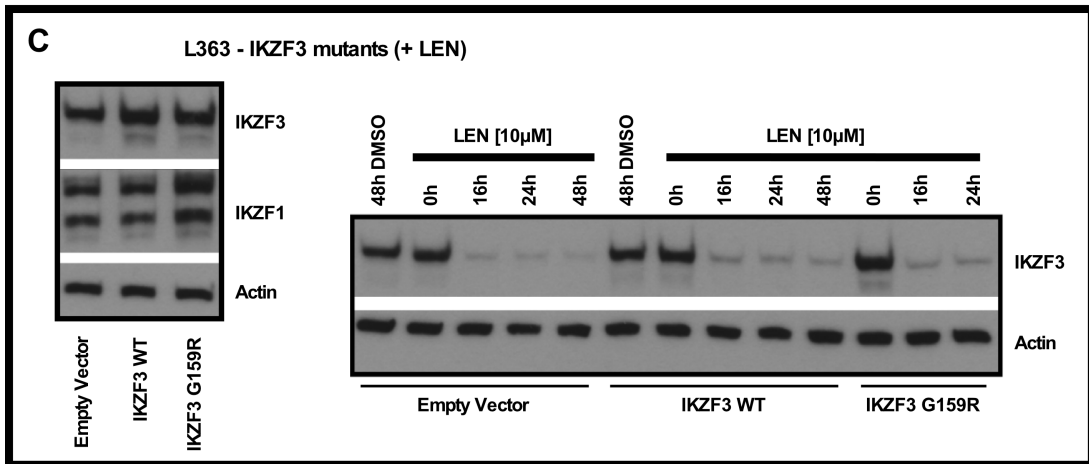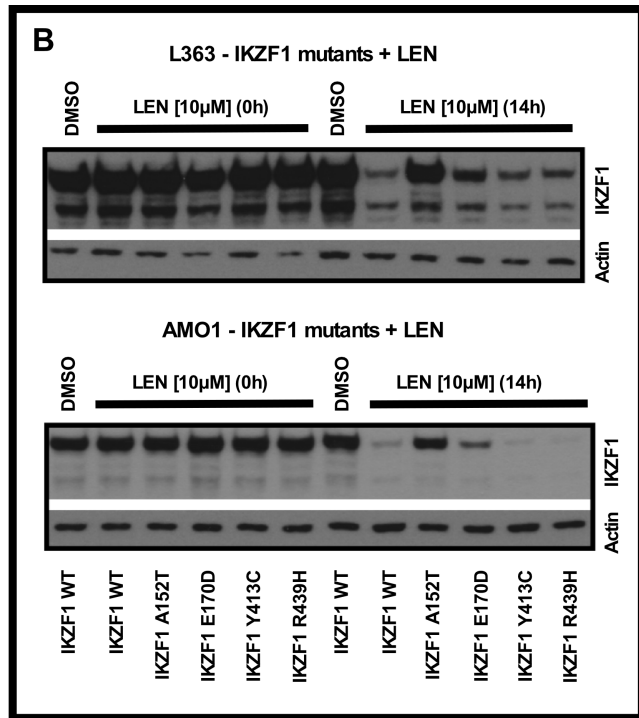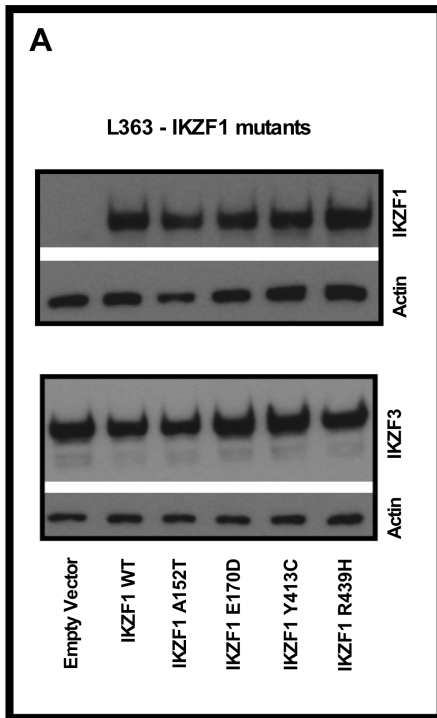
gene	Patient id	Cohort	Timepoint	IMID treated	IMID refractory/relapse	Chr	position	reference	genotype	function	VRF (%)	Baseline VRF (%)	previous timepoint VRF (%)	aa change	Predicted AAG SDM	Outcome SDM
IKZF3	176	M3P	Untreated	-	-	chr17	37933948	C	T	Missense	54	-	-	S118N	-	-
CUL4B	459	M3P	Untreated	-	-	chrX	119666359	-	T/G	Missense	50	-	-	D804A	-	-
CUL4B	MMRF_1796_1_BM	MMRF	Untreated	-	-	chr3	3215867	G	C	Missense	42	-	-	P85S	-0,63	Reduced stability
CRBN	MMRF_2305_1_BM	MMRF	Untreated	-	-	chr3	3215762	C	A	Missense	10,4	-	-	F120V	-1,54	Reduced stability
CRBN	MMRF_2402_1_BM	MMRF	Untreated	-	-	chr3	3192592	G	A	Missense	28,1	-	-	T429I	-	-
CRBN	MMRF_2754_1_BM	MMRF	untreated	-	-	chr3	3194191	C	T	Missense	29,5	-	-	C366Y	0,09	Increased stability
CUL4B	MMRF_2118_1_BM	MMRF	Untreated	-	-	chrX	119672540	T	A	Missense	5,5	-	-	K627N	-	-
CUL4B	MMRF_2336_1_BM	MMRF	Untreated	-	-	chrX	119669779	A	G	Missense	31,3	-	-	I707T	-	-
CUL4B	MMRF_2746_1_BM	MMRF	Untreated	-	-	chrX	119694456	G	T	Missense	23,6	-	-	A31D	-	-
DDB1	MMRF_1327_1_BM	MMRF	Untreated	-	-	chr11	61070587	G	T	Missense	6,6	-	-	E958A	0,27	Increased stability
DDB1	MMRF_1602_1_BM	MMRF	Untreated	-	-	chr11	61096942	C	A	Missense	4,5	-	-	D148Y	-0,09	Reduced stability
DDB1	MMRF_2041_1_BM	MMRF	Untreated	-	-	chr11	61070086	G	A	Missense	53	-	-	S1027L	1,27	Increased stability
DDB1	MMRF_2734_1_BM	MMRF	untreated	-	-	chr11	61081591	A	T	Missense	53,7	-	-	W561R	-0,92	Reduced stability
DDB1	MMRF_2734_1_BM	MMRF	Untreated	-	-	chr11	61081602	G	C	Missense	56,8	-	-	A557G	-1,57	Reduced stability
IKZF1	MMRF_1725_1_BM	MMRF	Untreated	-	-	chr7	50467856	C	T	Missense	35,8	-	-	S364L	-	-
IKZF3	MMRF_1725_1_BM	MMRF	Untreated	-	-	chr17	37933970	G	C	Missense	50	-	-	L254V	-	-
IKZF3	MMRF_1721_1_BM	MMRF	Untreated	-	-	chr17	37945581	C	G	Missense	32,5	-	-	Q213H	-	-
IKZF3	MMRF_1796_1_BM	MMRF	Untreated	-	-	chr17	37945581	C	G	Missense	52,4	-	-	Q213H	-	-
IKZF3	MMRF_1986_1_BM	MMRF	Untreated	-	-	chr17	37944581	C	G	Missense	10	-	-	Q213H	-	-
CRBN	299	M3P	Untreated	-	-	chr3	3195647	A	A/C	Missense	45	-	-	N316K	0,19	Increased stability
CUL4B	347	M3P	Untreated	-	-	chrX	119691847	G	G/C	Missense	45	-	-	L220V	-	-
IKZF1	278	M3P	Untreated	-	-	chr17	37934006	T	T/C	Missense	26	-	-	R242G	-	-
CUL4B	445	M3P	Untreated	-	-	chrX	119664085	-	C/G	Missense	32	-	-	E840Q	-	-
CUL4B	394	M3P	untreated	-	-	chrX	119691895	C	C/G	Splice_Site	5	-	-	G204_splice	-	-
IKZF3	355	M3P	untreated	-	-	chr17	37922121	CAT	CAT/C	Frame_Shift_Del	40	-	-	M484fs	-	-
IKZF3	MMRF_1963_1_BM	MMRF	Untreated	-	-	17	37922121	CAT	C	Frame_Shift_Del	48,1	-	-	M484fs	-	-
IKZF3	MMRF_1832_1_BM	M3P	untreated	-	-	17	37922133	G	GA	Frame_Shift_Del	46,8	-	-	G481fs	-	-
IKZF3	MMRF_2168	MMRF	untreated	-	-	17	37933954	A	G	Missense	91	96,3	-	L259S	-	-
CRBN	MM-0550-Tumor	Lohr	Untreated	-	-	chr3	3190788	C	T	Missense	48,7	-	-	R111Q	-0,01	Reduced stability
IKZF3	MM-0547-Tumor	Lohr	Untreated	-	-	chr17	35175897	T	C	Missense	12,4	-	-	Y401C	-	-
IKZF1	MMRF2787	MMRF	untreated	-	-	chr7	50444493	T	A		-	-	-	G141_splice	-	-